ADVANCED FUNCTIONAL MATERIALS
www.afm-journal.de

Analyzing Electronic Excitations and Exciton Binding Energies in Y6 Films

*Sahar Javaid Akram, Sophie Meißner, and Stephan Kümmel**

The Y6 molecule is one of the most promising non-fullerene acceptors. Based on first-principles calculations, this paper analyzes how the separation of an electronic excitation into electron and hole densities is influenced by the interaction between different Y6 molecules. By calculating the optical and the fundamental gaps of ensembles of Y6 molecules that realistically represent a film, their corresponding exciton binding energies are obtained. The combination of range separation, optimal tuning, and dielectric screening endows the presented density functional theory calculations with predictive power. The calculations reveal that the electronic excitations, characterized as electron–hole pairs via their natural transition orbitals, spread across multiple Y6 molecules. A distinct decrease in the exciton binding energy is correlated to a notable charge separation, and the exciton binding energy saturates in ensembles of six to seven Y6 molecules at ≈0.25 electronvolt (eV). These findings contribute to explaining the efficient charge separation in films of Y6. They also give a guideline for the number of molecules that theoretical models should take into account when they aim at a realistic description of charge separation.

1. Introduction

The Y6 molecule is the paradigm non-fullerene acceptor.[1] It is an attractive material for organic solar cells as its π–π molecular stacking in spin-coated films promotes delocalized exciton formation, reduced recombination loss, and high charge mobility.[2] The quest for understanding these properties and exploiting them in organic photovoltaic devices keeps spurring intense and successful research efforts.[3]

Understanding the interplay between structural properties, relative orientation, electronic excitations, and charge transfer characteristics in films of Y6 is crucial. While a lot of understanding has been gained already, charge separation, a decisive first step in converting light into electrical energy,[4] has not yet been fully understood. In this study, we calculate from first principles the electronic excitations of ensembles of Y6 molecules that realistically represent the structure of a Y6 film. Our results demonstrate that the lowest excitation is of charge-transfer character, and the electron and hole densities typically spread out over up to six Y6 molecules. In line with this relatively large electron–hole separation, our calculations yield relatively low exciton binding energies of ≈0.3 eV. This value is close to the experimental result. Our calculations thus offer an explanation for the efficient charge separation in Y6 systems. They can also be interpreted as a hint that structural control over the range of about six molecules in films of Y6 can contribute to controlling exciton dissociation. Furthermore, the results are of relevance for the understanding and setup of theoretical models that aim at describing films of Y6. Previous studies showed that excitations can spread over at least two to three Y6 molecules,[2,5] and highlighted the importance of the proper description of charge-transfer excitations.[6] Thanks to the high-level molecular dynamics (MD) simulations performed by Kupgan et al.[7] a realistic atomistic picture of the molecular arrangement in films of Y6 is known. Our calculations based on these coordinates show that taking into account approximately six Y6 molecules is required for a realistic description of the electronic excitations in films of Y6.

2. Theoretical and Computational Approach

The basic idea of our work is to systematically investigate the delocalization of the electronic excitations and the charge-separation process in Y6 by starting from one Y6 molecule and then systematically taking into account an increasing number of neighboring Y6 molecules. For each of these ensembles of increasing size, we calculate the fundamental and the optical gap, and from their difference the exciton binding energy (E_b). To ensure that our ensembles of Y6 molecules realistically represent the geometry and relative arrangement that Y6 molecules have in a film, we make use of the MD coordinates that were obtained by Kupgan et al.[7] From these coordinates, we selected several ensembles of Y6 molecules of increasing size and calculated the fundamental gap using density functional theory (DFT), and the

S. J. Akram, S. Meißner, S. Kümmel
Theoretical Physics IV
University of Bayreuth
95447 Bayreuth, Germany
E-mail: stephan.kuemmel@uni-bayreuth.de

The ORCID identification number(s) for the author(s) of this article can be found under https://doi.org/10.1002/adfm.202419236

DOI: 10.1002/adfm.202419236

optical gap using time-dependent (TD) DFT. We rely on an optimally tuned range-separated hybrid (OT-RSH) functional.[8] This approach is known for its predictive accuracy.[9] We analyze the charge transfer character of the excitations via the natural transition orbital (NTO) decomposition.[10] In order to take into account the effects of the film environment beyond the ensemble of molecules that we study explicitly, we complement the analysis by using the screened range-separated hybrid (sRSH) approach,[11] in combination with a polarizable continuum model (PCM).[12] How this general idea is realized in practice is explained in the following.

An important aspect of our study is the use of the OT-RSH approach. The range-separation divides the Coulomb operator "$1/r_{12}$" in the exchange integral of the exchange-correlation energy into long (Hartree–Fock; HF) & short (generalized gradient approximations; GGA) range parts according to the expression:[13]

$$\frac{1}{r_{12}} = \frac{\alpha + \beta \,\mathrm{erf}\left(\omega r_{12}\right)}{r_{12}} + \frac{1 - \left(\alpha + \beta \mathrm{erf}\left(\omega r_{12}\right)\right)}{r_{12}} \quad (1)$$

Here, r_{12} denotes the inter-electron distance, while erf is the standard error function. α defines the percentage of short-range HF exchange, whereas $\alpha + \beta$ represents the percentage of HF exchange in the long-range limit. The decisive parameter is ω, which is the range-separation parameter controlling the division of $1/r_{12}$ into long-range & short-range components. Thus, the expression for the exchange-correlation energy of the RSH functional reads:

$$E_{xc}^{RSH} = \alpha E_{x,HF}^{SR} + (1-\alpha)\, E_{x,GGA}^{SR} + (\alpha+\beta)\, E_{x,HF}^{LR} + (1-\alpha-\beta)\, E_{x,GGA}^{LR} + E_c^{GGA} \quad (2)$$

LR & SR represent the long-range and short-range Coulomb repulsions from Equation (1).

For the optimal tuning (OT) of the RSH functional, two constraints were imposed. The first one is $\alpha + \beta = 1$,[14] to ensure the correct asymptotic behavior (1/r) of the exchange-correlation potential for finite systems in vacuum. Thus, the energy expression for the RSH functional reduces to:

$$E_{xc}^{RSH} = \alpha E_{x,HF}^{SR} + E_{x,HF}^{LR} + (1-\alpha)\, E_{x,PBE}^{SR} + E_c^{PBE} \quad (3)$$

Here, we used the Perdew-Burke-Ernzerhof (PBE) GGA for the semi-local component and the usual value of $\alpha = 0.2$.[15] The second constraint is to optimally tune the range-separation parameter ω by minimizing the quantity $J(\omega)$,[16]

$$J\ (\omega) = \left[\varepsilon_{HOMO(N)}\,(\omega) + IP\,(\omega)\right]^2 + \left[\varepsilon_{HOMO(N+1)}\,(\omega) + EA\,(\omega)\right]^2 \quad (4)$$

as suggested by Koopmans' theorem:[17]

$$\varepsilon_{HOMO} = E\,(N) - E\ (N-1) = -IP \quad (5)$$

Here, E(N) is the ground state energy of the system with N electrons, and E(N-1) is the ground state energy of the corresponding cation. IP and EA are the ionization potential and the electron affinity of the system, while $\boldsymbol{\varepsilon_{HOMO}}$ and $\boldsymbol{\varepsilon_{LUMO}}$ are the HOMO and LUMO eigenvalues, respectively. Minimizing J to a value close to zero ensures that the frontier eigenvalues obtain physical meaning such that the generalized Kohn–Sham HOMO-LUMO gap becomes a good approximation to the fundamental gap ($\boldsymbol{E_g = IP - EA}$).[8,17,18] Though optimal tuning has been extremely successful, it has the shortcoming that repeated tuning for systems of increasing size tends to yield systematic errors, as the resulting functional becomes increasingly semi-local.[19] Luckily, in our study here we can sidestep this problem because our systems of increasing size are all built from the same molecule, Y6. Therefore, tuning ω once for one molecule sets the proper scale for the range separation, and this value ($\omega = 0.127\mathrm{bohr}^{-1}$) can then be used for all ensembles. This procedure has, e.g., been used successfully for biological light-harvesting systems,[20] and its reliability for Y6 is confirmed in tests that we discuss in the supplementary material. Using this OT-RSH functional, we calculated the exciton binding energies (E_b) for ensembles of Y6 molecules of increasing size, and characterized the charge transfer characteristics of the involved electronic excitations via their NTOs. Our calculations and visualization relied on QChem and the GaussView 6 software.[21] The number of Y6 molecules that can explicitly be included in such TDDFT calculations is, however, limited. Therefore, we complement the OT-RSH calculations for the bare ensembles of Y6 molecules by additional calculations, in which the dielectric effects of the further, more distant parts of the film environment are taken into account. The method of choice for this is the sRSH-PCM approach. The first use of the sRSH methodology demonstrated that it can capture the effect of gap renormalization.[11] In a second and independent line of development, the combination of RSH and PCM was demonstrated to be able to describe charge-transfer excitations reliably,[22] and the intricacies of the combination of OT-RSH and PCM were pointed out.[19b,23] Further works established that the combination of sRSH, optimal tuning, and PCM is a powerful technique that can yield very accurate results, and it has been successfully used for studying a variety of problems in which the reliable prediction of band gaps or charge-transfer excitations is important;[12b,16b,24] see ref. [13a] for a review. In our work here, we relied on the implementation of the sRSH-PCM approach in QChem,[21] which requires to provide the values for the static (ε_s) and the optical (ε_o) dielectric constant. Values for both have been reported in the literature ($\varepsilon_s = 3.5$[25] and $\varepsilon_o = 5.3$,[3b]) and we discuss our use of these numbers in the Supporting Information. The sRSH is based on the energy functional in which $\omega = 0.127$ bohr^{-1} was kept as established previously via OT. For the dielectric screening in Equation (6), it is reasonable to use the value of the optical dielectric constant as our aim is the calculation of the optical electronic excitations. The coefficient of long-range Fock exchange then is $\alpha + \beta = 1/\varepsilon_o$, and we used $\alpha = 0.3$, i.e., the value that has previously been suggested for molecules embedded in a condensed phase environment.[26]

$$E_{xc}^{sRSH} = \alpha E_{x,HF}^{SR} + \frac{1}{\varepsilon} E_{x,HF}^{LR} + (1-\alpha)\, E_{x,PBE}^{SR} + \left(1 - \frac{1}{\varepsilon}\right) E_{x,PBE}^{LR} + E_c^{PBE} \quad (6)$$

One might wonder whether the OT-RSH or the sRSH-PCM approach is more suitable for describing the situation that is of

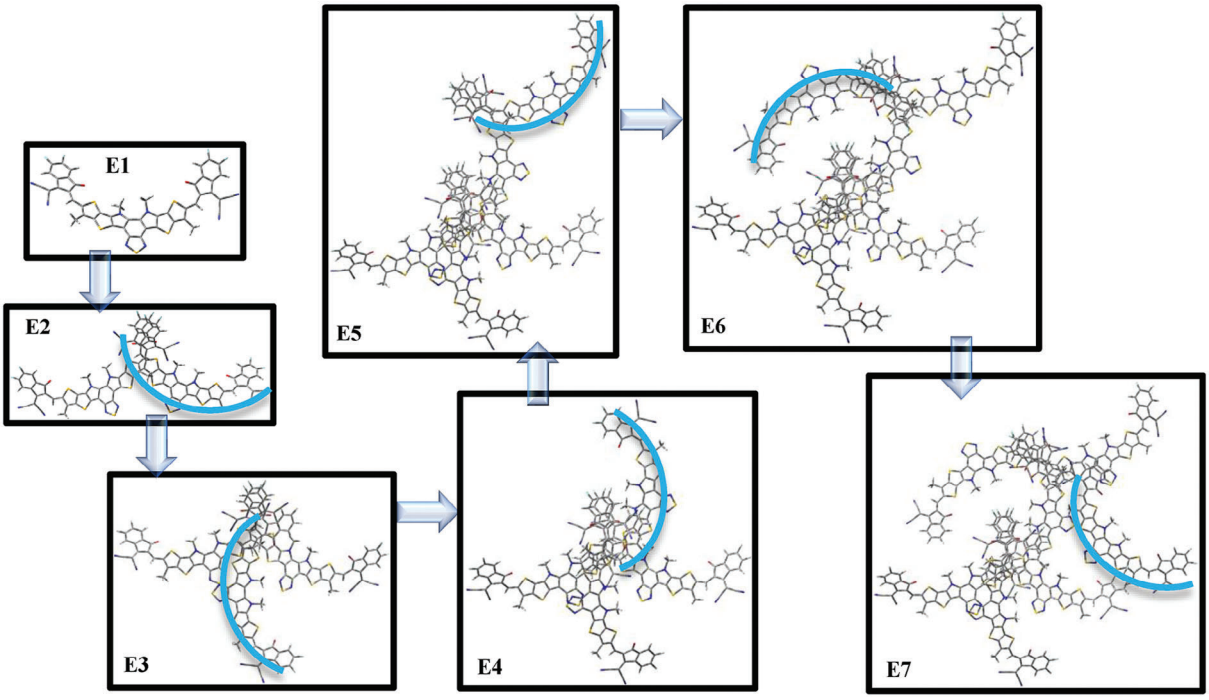

Figure 1. Ensembles of Y6 molecules present in Set A. The blue curve depicts the placement of the added Y6 molecule in the ensemble.

interest in our study, i.e., molecules that are part of a film. Therefore, it is important to note that the character of the electronic excitations is already described correctly by the OT-RSH calculations, as one can see by comparing the NTOs obtained in Section 5 on the one hand, to the NTOs from the sRSH-PCM calculations reported in Section 6 and the Supporting Information on the other hand. Thus, our conclusions about the nature of the excitations are independent of the computational details, and the inclusion of the screening does not change the character of the excitations, but just lowers the exciton binding energy. This confirms our strategy of explicitly including the most relevant parts of the film environment into our TDDFT calculations via the ensembles of increasing size. A detailed comparison of the numerical results obtained with the OT-RSH and the sRSH-PCM approaches is given in the Tables S6–S8 (Supporting.Information).

Finally, in tests that we report in detail in the Figure S1 in the Supporting.Information, we established that the 6–311G basis set is a reliable choice for our study.

3. Construction of the Molecular Ensembles

We constructed the Y6 ensembles for our study based on the coordinates of 200 Y6 molecules that were reported by Kupgan et al.[7] Within the complete simulation box containing the 200 molecules we selected a region in which the Y6 molecules exhibit directional face-on stacking and numerous close contacts, i.e., are representative of favorable conditions in a film. A close contact is defined as an intermolecular distance of less than 4Å between two molecules, implying a greater degree of face-on overlapping, as detailed in Ref.[7] From the molecules within this carefully chosen region, we created ensembles of increasing size according to the following protocol: We began by selecting one Y6 molecule from the center of the region. We designate it as E1. The nearest neighboring Y6 molecule to E1 was then added to form the E2 ensemble. This process was repeated, with each new ensemble incorporating an additional neighboring Y6 molecule, until we established a complete series of ensembles from E1 to E7. We did not go beyond seven Y6 molecules as this is the upper limit for the system size that we could cover in the TDDFT calculations with OT-RSH or sRSH-PCM, respectively. This first set of ensembles from E1 to E7 is referred to as Set A.

In order to make sure that our conclusions are not biased by the specific arrangement of molecules in Set A, we repeated the above-described procedure of creating ensembles of increasing size within a different region of the complete simulation box of 200 molecules that did not overlap with the region from which Set A was selected. In this way, we generated a set of ensembles that we refer to as Set B. Following the same procedure once more, we generated a third set of ensembles, called Set C.

To reduce computational costs and improve clarity in the visualization of the Y6 molecules within the ensembles, we substituted their long alkyl chains with methyl ones (see the Supporting Information for details). The substituted ensembles of Set A are shown in **Figure 1**, while those of Sets B and C are displayed in Figure S4 (Supporting Information). As discussed in detail in the Supporting Information, the substitution increases the exciton binding energies by ≈0.1 eV, but has hardly any effect otherwise.

4. Exciton Binding Energies of the Y6 Ensembles (OT-RSH)

In a single-particle picture, the exciton binding energy is interpreted as the energy required to dissociate a bound electron–hole pair into separate charges. More generally, the exciton binding

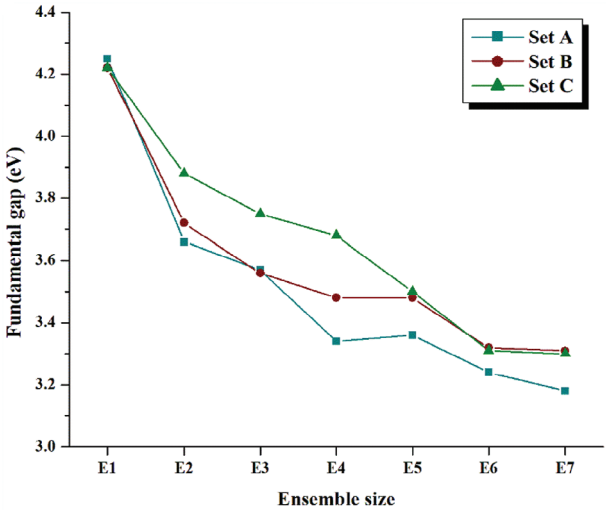

Figure 2. The Fundamental gap E_g as calculated for ensembles of Y6 molecules of increasing size. (OT-RSH calculations for ensembles in vacuum as described in the main text.).

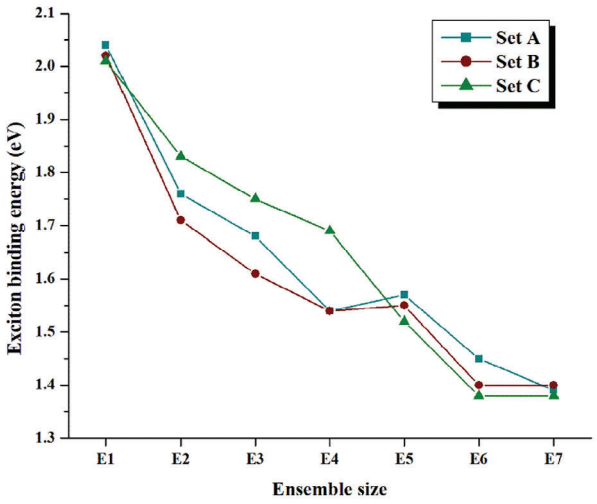

Figure 3. The exciton binding energy for ensembles of increasing size. In all three sets, E_b clearly decreases with increasing system size. (OT-RSH calculations for ensembles in vacuum as described in the main text.).

energy for a many electron system is defined as the difference between the fundamental gap and the optical gap, i.e.,

$$E_b = E_g - E_{opt} \tag{7}$$

For all ensembles in the three sets A, B, and C, we calculated E_b based on Equation (7). To this end, we first calculated for each of the ensembles the fundamental gap E_g as the difference between the ionization potential ($IP = E_{cation} - E_{neutral}$) and the electron affinity ($EA = E_{neutral} - E_{anion}$) of the ensemble. Here, $E_{neutral}$ is the ground state energy of the neutral system, while E_{cation} and E_{anion} are the ground state energies of its cation and anion, respectively. **Figure 2** depicts E_g for E1 to E7 in each of the sets A, B, and C, respectively (detailed data in Table S1, Supporting.Information). One clearly observes a decreasing trend in all sets, as expected for increasing delocalization. The delocalization is also reflected in a reduced energetic difference between the HOMO and LUMO eigenvalues, i.e., a narrowing single-particle gap that we observe in our calculations.

The second observable needed for the calculation of E_b, the optical gap E_{opt}, is defined as the energy difference between the first excited state (S_1) and the ground state (S_0). E_{opt} was obtained for each of the ensembles from the optical spectrum (Figure S5, Supporting.Information) which we calculated using TDDFT as described in Section 2. From the obtained fundamental and optical gaps, we then calculated the E_b value for every ensemble in the Sets A, B, and C. The obtained exciton binding energies are depicted in **Figure 3** (detailed data in Table S2, Supporting.Information), which thus visualizes the first central result of our work: Figure 3 shows how E_b changes as the number of Y6 molecules in the considered ensembles increases. It reveals the very clear trend that E_b decreases as the number of molecules in the ensemble increases from E1 to E7. This demonstrates that in order to obtain a realistic picture of the exciton binding energy in Y6, it is clearly necessary to go beyond considering just two or three molecules. This observation is made for all three sets A, B, and C. It is thus a general observation that does not result from just one particular arrangement of molecules

A further relevant observation is that in all three sets, a clearly decreasing value of E_b is observed for the Y6 ensembles E2 to E4. However, from E5 to E7, the E_b values appear to converge, indicating that Y6 ensembles with a larger number of molecules tend to exhibit similar E_b values irrespective of their molecular arrangements. Finally, a significant drop in E_b is observed at E6, and one sees a saturation of E_b at E7. These trends fall well in line with the behavior that one would expect for exciton charge separation. In the following, we therefore analyze the spatial structure of the excitations in the different ensembles.

5. Natural Transition Orbitals of the Y6 Ensembles (OT-RSH)

NTOs[10] can allow to obtain an impression of the charge redistribution that is associated with a given excitation, and the corresponding electron and hole orbitals can visualize, e.g., the charge-transfer character of an excitation. They are therefore an ideal tool for analyzing the Y6 ensembles. **Figure 4** shows the exciton binding energies obtained for set A together with the electron (particle) and hole orbitals (NTOs) of the first electronic excitation. To avoid overcrowding the figure, we only show the NTOs for the three ensembles E2, E5, and E7, while the NTOs of the other ensembles are displayed in Figure S6 (Supporting.Information). These three ensembles were chosen because they characteristically show how the charge separation depends on the system size and relates to the E_b values. One sees in Figure 4 that in the case of the smallest ensemble E2, the hole density is spread across the entire system and strongly overlaps with the electron density. Thus, the drop in exciton binding energy from E1 to E2 is associated with an increase in delocalization, but not with a clear charge separation.

As the number of Y6 molecules increases further, electron and hole densities can spread out further. The NTOs of E5 are a typical example of this intermediate situation: Electron and hole

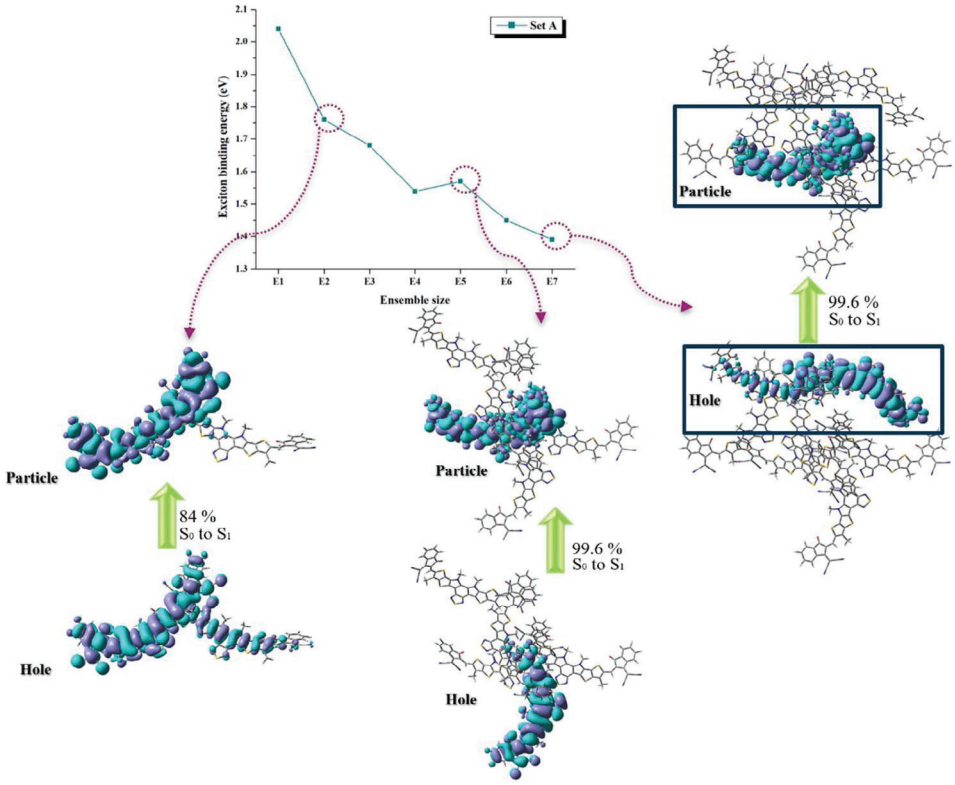

Figure 4. Exciton binding energies for the ensembles in Set A together with the NTOs for the first excitations of the ensembles E2, E5, and E7. The NTOs of these ensembles paradigmatically illustrate the transition from partial to complete charge separation with increasing system size. (OT-RSH calculations for ensembles in vacuum as described in the main text.).

densities tend to separate, but there is still a substantial overlap between the two in the center of the system. The situation is very similar for E3 and E4, as seen in Figure S6 (Supporting.Information). A clear charge separation is first observed at E6 (Figure S6, Supporting.Information), and slightly increases further when going from E6 to E7. As seen in Figure 4, electron and hole densities are well separated and localized in different regions once the ensemble E7 has been reached. When one returns to Figure 3, and complements it with Figures S7 and S8 (Supporting.Information), one sees that the situation is qualitatively very similar in the other sets B and C. In sets B and C, some aspects are even a bit clearer: In B and C, the exciton binding energy does not change anymore when going from E6 to E7, and this is reflected in electron and hole densities that do not change anymore. For Set C, the situation is particularly transparent: The gradual decrease of E_b from E1 to E4 that is seen in Figure 3 is accompanied by a gradually increasing charge separation seen in the NTOs (Figure S8, Supporting.Information), whereas the pronounced drops of E_b beyond E4 are accompanied by more substantial changes and a spatial separation of the NTOs.

These results demonstrate that in order to capture the charge separation that typically goes along with the optical excitation of a film it is necessary to look at more than just two Y6 molecules. In all cases that we studied, taking into account six molecules was sufficient for obtaining a trustworthy picture of the excitation. This result can serve as a guideline for the size that supramolecular models should have in order to capture the decisive aspects of the electronic structure of films of Y6. However, an effect that the calculations presented so far do not yet take into account is the influence that further, more distant molecules of the film have on the excitation energies. Though not directly involved in the electronic excitations, the surrounding film represents a dielectric environment that creates a different situation than the one of Y6 ensembles in a vacuum that we studied so far. We study this influence in the following section.

6. Exciton Binding Energies of Embedded Y6 Ensembles (sRSH-PCM)

As discussed in Section 2, the effects of a dielectric surrounding can be taken into account with the sRSH-PCM approach. The detailed data for the fundamental gaps, the optical gaps, and the exciton binding energies obtained with this strategy are listed in Tables S2–S4 (Supporting.Information) for sets A, B, and C, respectively. **Figure 5** visualizes the central result, the exciton binding energies. We note in passing that in Set B, the value for E5 comes with an uncertainty as discussed in the Supporting Information. Two decisive insights emerge from Figure 5. The first is that quantitatively, there is a substantial change: Taking into account the film environment via the sRSH-PCM approach lowers the exciton binding energies pronouncedly. The second is that the trend of how the exciton binding energy changes as a function of the ensemble size is qualitatively quite similar in the OT-RSH and the sRSH-PCM calculations. This second finding is

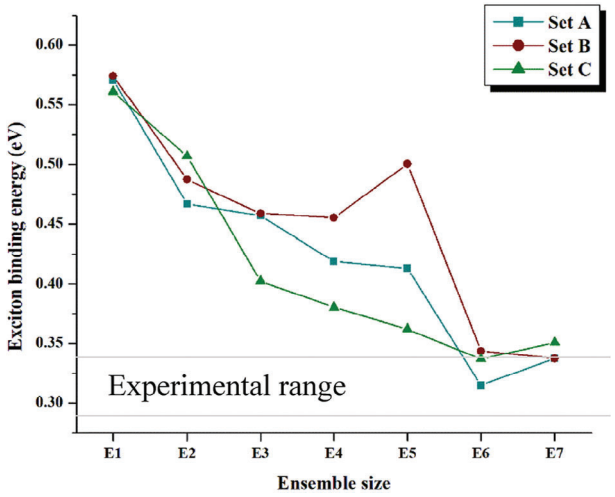

Figure 5. Exciton binding energies for the three sets of Y6 ensembles as obtained in the sRSH-PCM calculations that take into account the screening effects due to the film environment. The two horizontal lines indicate the range in which the experimental results[27] are found.

underlined further by the observation that the NTOs that one finds in the sRSH-PCM calculations for the Y6 ensembles, see Figure S9 (Supporting.Information), are extremely similar to the NTOs that were found for the ensembles in the OT-RSH calculations. This confirms that the trend of charge separation is already well described in the bare ensembles, and the additional screening in the sRSH-PCM calculations just lowers the exciton binding energies, in agreement with one's intuitive expectation. Finally, we compare the calculated exciton binding energies to the available experimental data for Y6 films.[27] The range for the experimental results is indicated in Figure 5 by the two horizontal lines. The important observation is that with the increasing size of the ensemble, the calculated values for E_b approach the experimental range, and for E6 and E7, the exciton binding energies are at the upper boundary of the experimental range for all three sets of ensembles. When one takes into account that the substitution of the alkyl chains by methyl groups increased the exciton binding energies by ≈0.1 eV, cf. Section 3 and Figure S3 (Supporting.Information), one sees that the calculations agree remarkably well with the experimentally determined exciton binding energies. Furthermore, the importance of the interaction between Y6 molecules in a film that our results show is well in line with very recent experimental findings.[3d]

7. Conclusion

In this study, we investigated the charge separation within different ensembles of Y6 molecules that represent different possible molecular geometries in a film. We analyzed the fundamental and optical gaps, the exciton binding energies, and the natural transition orbitals associated with the electronic excitations under two distinct environmental conditions. First, using the OT-RSH method, we studied the ensembles as such. Then, we employed the sRSH-PCM approach to study the impact of the environmental screening on the exciton binding energies and charge transfer characteristics. The nature of the electronic excitations as described by the NTOs was very similar in both approaches. The calculations showed that the first excitation spreads over many molecules, and taking into account just one or two neighbors is not sufficient for obtaining a realistic picture of the situation in a film. However, in all cases that we studied, the exciton binding energy converged when about six neighboring Y6 molecules were included in the calculations, and this convergence of the energy was accompanied by a well-established charge separation. When the screening effect of the film environment was taken into account, the obtained exciton binding energies were in close agreement with the experimentally obtained values. This demonstrates that TDDFT with the combination of range separation, optimal tuning, and screening can yield detailed insight into the first step of the process that converts light into separated charges in films of Y6. Our results contribute to explaining the low exciton binding energy that is observed in films of Y6: The delocalization of the initially generated electron–hole pair over many molecular units facilitates the charge separation step.

Supporting Information

Supporting Information is available from the Wiley Online Library or from the author.

Acknowledgements

The authors thank Dr. Sadisha Nanayakkara and Prof. Jean-Luc Brédas from the University of Arizona for making available to the coordinates of the Y6 molecules from the molecular dynamics simulations of ref. [7] and the authors thank Anna Köhler for discussions. The authors acknowledge financial support by the Deutsche Forschungsgemeinschaft via IRTG 2818 (OPTEXC, project grant number 492723217), and by the Bavarian State Ministry of Science via the Solar Technologies go Hybrid research program. The calculations were performed on the emil-Cluster of the Bayreuth Center for High Performance Computing, supported by the Deutsche Forschungsgemeinschaft via DFG grant number 422127126.

Open access funding enabled and organized by Projekt DEAL.

Conflict of Interest

The authors declare no conflict of interest.

Author Contributions

S.J.A and S.K. conceptualized the work. S.J.A did all the calculations, and prepared all figures and tables in discussion with S.K. S.M. provided technical support and data for the optimal tuning. S.K. supervised the project. S.J.A. wrote the first draft of the manuscript. S.K. and S.J.A. together wrote the final version of the manuscript. All authors discussed the final results and the final manuscript.

Data Availability Statement

The data that support the findings of this study are available in the supplementary material of this article.

Keywords

density functional theory, exciton binding energies, optimal tuning, screened range separated hybrid, Y6 molecules

Received: October 11, 2024
Revised: February 12, 2025
Published online:

[1] a) J. Yuan, Y. Zhang, L. Zhou, G. Zhang, H. L. Yip, T. K. Lau, X. Lu, C. Zhu, H. Peng, P. A. Johnson, M. Leclerc, Y. Cao, J. Ulanski, Y. Li, Y. Zou, *Joule* **2019**, *3*, 1140; b) W. Liu, X. Xu, J. Yuan, M. Leclerc, Y. Zou, Y. Li, *ACS Energy Lett.* **2021**, *6*, 598; c) D. Luo, W. Jang, D. D. Babu, M. S. Kim, D. H. Wang, A. K. K. Kyaw, *J. Mater. Chem. A* **2022**, *10*, 3255.
[2] G. Zhang, X. K. Chen, J. Xiao, P. C. Chow, M. Ren, G. Kupgan, X. Jiao, C. C. Chan, X. Du, R. Xia, Z. Chen, J. Yuan, Y. Zhang, S. Zhang, Y. Liu, Y. Zou, H. Yan, K. S. Wong, V. Coropceanu, N. Li, C. J. Brabec, J. L. Bredas, H. L. Yip, Y. Cao, *Nat. Commun.* **2020**, *11*, 3943.
[3] a) S. Giannini, D. J. Sowood, J. Cerdá, S. Frederix, J. Grüne, G. Londi, T. Marsh, P. Ghosh, I. Duchemin, N. C. Greenham, K. Vandewal, G. D'Avino, A. J. Gillet, D. Beljonne, *Mater. Today* **2024**, *80*, 308; b) P. A. Hume, M. B. Price, J. M. Hodgkiss, *JACS Au* **2024**, *4*, 1295; c) D. Kroh, S. Athanasopoulos, V. Nádaždy, F. J. Kahle, H. Bässler, A. Köhler, *Adv. Funct. Mater.* **2024**, *34*, 2302520; d) S. Mahadevan, T. Liu, S. M. Pratik, Y. Li, H. Y. Ho, S. Ouyang, X. Lu, H. L. Yip, P. C. Chow, J. L. Brédas, V. Coropceanu, S. K. So, S. W. Tsang, *Nat. Commun.* **2024**, *15*, 2393.
[4] J. L. Brédas, J. E. Norton, J. Cornil, V. Coropceanu, *Acc. Chem. Res.* **2009**, *42*, 1691.
[5] a) J. Zhang, Y. Xiang, S. Zheng, *New J. Chem.* **2021**, *45*, 12247; b) Q. Si, M. Lian, Y. Zhao, *J. Chin. Chem. Soc.* **2023**, *70*, 625; c) L. Zhu, J. Zhang, Y. Guo, C. Yang, Y. Yi, Z. Wei, *Angew. Chem.* **2021**, *133*, 15476.
[6] J. L. Lan, X. N. Liu, C. N. Xiao, M. Y. Sui, G. Y. Sun, *J. Photochem. Photobiol. A Chem.* **2024**, *456*, 115821.
[7] G. Kupgan, X. Chen, J. L. Bredas, *Mater. Today Adv.* **2021**, *11*, 100154.
[8] L. Kronik, T. Stein, S. Refaely-Abramson, R. Baer, *J. Chem. Theory Comput.* **2012**, *8*, 1515.
[9] H. Phillips, Z. Zheng, E. Geva, B. D. Dunietz, *Org. Electron.* **2014**, *15*, 1509.
[10] R. L. Martin, *J. Chem. Phys.* **2003**, *118*, 4775.
[11] S. Refaely-Abramson, S. Sharifzadeh, M. Jain, R. Baer, J. B. Neaton, L. Kronik, *Phys. Rev. B:Condens. Matter Mater. Phys.* **2013**, *88*, 081204.
[12] a) L. R. Franco, C. Marchiori, C. M. Araujo, *J. Chem. Phys.* **2023**, *159*, 204110; b) S. Bhandari, M. S. Cheung, E. Geva, L. Kronik, B. D. Dunietz, *J. Chem. Theory Comput.* **2018**, *14*, 6287.
[13] a) L. Kronik, S. Kümmel, *Adv. Mater.* **2018**, *30*, 1706560; b) A. K. Manna, S. Refaely-Abramson, A. M. Reilly, A. Tkatchenko, J. B. Neaton, L. Kronik, *J. Chem. Theory Comput.* **2018**, *14*, 2919; c) T. Leininger, H. Stoll, H. J. Werner, A. Savin, *Chem. Phys. Lett.* **1997**, *275*, 151; d) D. A. Egger, S. Weissman, S. Refaely-Abramson, S. Sharifzadeh, M. Dauth, R. Baer, S. Kümmel, J. B. Neaton, E. Zojer, L. Kronik, *J. Chem. Theory Comput.* **2014**, *10*, 1934.
[14] S. Refaely-Abramson, S. Sharifzadeh, N. Govind, J. Autschbach, J. B. Neaton, R. Baer, L. Kronik, *Phys. Rev. Lett.* **2012**, *109*, 226405.
[15] J. Yang, S. Falletta, A. Pasquarello, *npj Comput. Mater.* **2023**, *9*, 108.
[16] a) I. Tamblyn, S. Refaely-Abramson, J. B. Neaton, L. Kronik, *J. Phys. Chem. Lett.* **2014**, *5*, 2734; b) Z. Zheng, D. A. Egger, J. L. Bredas, L. Kronik, V. Coropceanu, *J. Phys. Chem. Lett.* **2017**, *8*, 3277; c) M. Srebro, J. Autschbach, *J. Phys. Chem. Lett.* **2012**, *3*, 576; d) T. Stein, L. Kronik, R. Baer, *J. Chem. Phys.* **2009**, *131*, 244119; e) T. Körzdörfer, J. L. Brédas, *Acc. Chem. Res.* **2014**, *47*, 3284.
[17] U. Salzner, R. Baer, *J. Chem. Phys.* **2009**, *131*, 231101.
[18] a) T. Vikramaditya, J. D. Chai, S. T. Lin, *J. Comput. Chem.* **2018**, *39*, 2378; b) T. Vikramaditya, S. T. Lin, *J. Comput. Chem.* **2017**, *38*, 1844; c) J. P. Perdew, M. Levy, *Phys. Rev. B* **1997**, *56*, 16021; d) S. Refaely-Abramson, R. Baer, L. Kronik, *Phys. Rev. B:Condens. Matter Mater. Phys.* **2011**, *84*, 075144.
[19] a) T. Körzdörfer, J. S. Sears, C. Sutton, J. L. Brédas, *J. Chem. Phys.* **2011**, *135*, 204107; b) T. B. de Queiroz, S. Kümmel, *J. Chem. Phys.* **2014**, *141*, 084303; c) M. Brütting, H. Bahmann, S. Kümmel, *J. Chem. Phys.* **2024**, *160*, 181101; d) S. Fürst, M. Kaupp, *J. Chem. Theory Comput.* **2023**, *19*, 3146.
[20] M. Brütting, J. M. Foerster, S. Kümmel, *J. Phys. Chem. Lett.* **2023**, *14*, 3092.
[21] a) S. Höfener, W. Klopper, *Chem. Phys. Lett.* **2017**, *679*, 52; b) R. Dennington, T. A. Keith, J. M. Millam, *Semichem Inc., Shawnee Mission, KS* **2016**, 143; c) Y. Shao, Z. Gan, E. Epifanovsky, A. T. Gilbert, M. Wormit, J. Kussmann, A. W. Lange, A. Behn, J. Deng, X. Feng, D. Ghosh, M. Goldey, P. R. Horn, L. D. Jacobson, I. Kaliman, R. Z. Khaliullin, T. Kuś, A. Landau, J. Liu, E. I. Proyonov, Y. M. Rhee, R. M. Richard, M. A. Rohrdanz, R. P. Steele, E. J. Sundstrom, L. Woodcock III, P. M. Zimmerman, D. Zuev, B. Albrecht, E. Alguire, et al., *Mol. Phys.* **2015**, *113*, 184.
[22] a) S. Zheng, H. Phillips, E. Geva, B. D. Dunietz, *J. Am. Chem. Soc.* **2012**, *134*, 6944; b) S. Zheng, E. Geva, B. D. Dunietz, *J. Chem. Theory Comput.* **2013**, *9*, 1125.
[23] O. S. Bokareva, G. Grell, S. I. Bokarev, O. Kühn, *J. Chem. Theory Comput.* **2015**, *11*, 1700.
[24] a) H. Sun, Z. Hu, C. Zhong, S. Zhang, Z. Sun, *J. Phys. Chem. C* **2016**, *120*, 8048; b) B. Joo, H. Han, E. G. Kim, *J. Chem. Theory Comput.* **2018**, *14*, 2823; c) S. Bhandari, B. D. Dunietz, *J. Chem. Theory Comput.* **2019**, *15*, 4305; d) H. Aksu, B. Maiti, M. Ptaszek, B. D. Dunietz, *J. Chem. Phys.* **2020**, *153*, 134111; e) C. Chakravarty, H. Aksu, B. Maiti, B. D. Dunietz, *J. Phys. Chem. A.* **2021**, *125*, 7625; f) R. V. Dantas Filho, T. B. de Queiroz, *J. Chem. Phys.* **2024**, *161*, 034109.
[25] X. Zhang, C. Li, J. Xu, R. Wang, J. Song, H. Zhang, Y. Li, Y. N. Jing, S. Li, G. Wu, J. Zhou, X. Li, Y. Zhang, X. Li, J. Zhang, C. Zhang, H. Zhou, Y. Sun, Y. Zhang, *Joule* **2022**, *6*, 444.
[26] K. Begam, S. Bhandari, B. Maiti, B. D. Dunietz, *J. Chem. Theory Comput.* **2020**, *16*, 3287.
[27] a) D. Neusser, B. Sun, W. L. Tan, L. Thomsen, T. Schultz, L. Perdigón-Toro, N. Koch, S. Shoaee, C. R. McNeill, D. Neher, S. Ludwigs, *J. Mater. Chem. C* **2022**, *10*, 11565; b) A. Sugie, K. Nakano, K. Tajima, I. Osaka, H. Yoshida, *J. Phys. Chem. Lett.* **2023**, *14*, 11412.